Synthesis, Characterization, and Self-Assembling Properties of New Amphiphilic Dendrons Bearing Branched TRIS-Derived Oligomers as Polar Head Groups

Stéphane Desgranges, Valentin Lacanau, Françoise Bonneté, Marine Soulié, Frédéric Bihel, Damien Bourgeois, Christiane Contino-Pépin

Synthesis, characterization and self-assembling properties of new amphiphilic dendrons bearing branched TRIS-derived oligomers as polar head groups

*Stéphane Desgranges, Valentin Lacanau, Françoise Bonneté, Marine Soulié, Frédéric Bihel, Damien Bourgeois, Christiane Contino-Pépin**

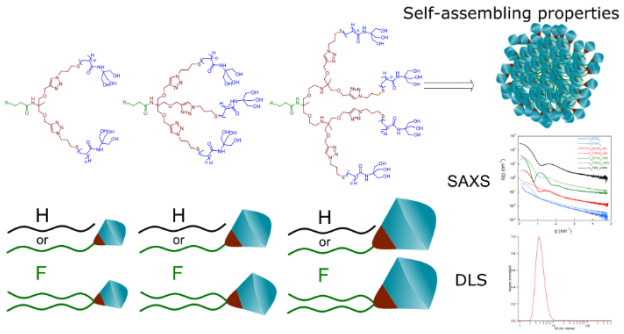

for Table of Contents use only

ABSTRACT

The synthesis and characterization of a new family of dendritic surfactants called Dendri-TAC is described. Two series of single or double-tailed surfactants containing hydrophobic hydrocarbon or fluorocarbon chains grafted onto Tris(hydroxymethyl)aminomethane (or TRIS)-derived oligomeric polar heads, via a copper (I)-mediated click reaction, have been prepared. A total of thirteen new dendritic surfactants have been obtained by grafting linear polyTRIS branches of variable average degree of polymerization (DPn) onto a single or double-tailed fluorinated or hydrocarbon chain of variable length, via a dendritic central scaffold of generation G_1 or G_2. Structural parameters of the surfactant assemblies in solution (radii of gyration (R_G), volume-weighted hydrodynamic radii (R_H) and aggregation numbers (N_{ag})) were assessed by small-angle X-ray scattering (SAXS) and dynamic light scattering (DLS). Overall,

regardless of their tree-like structure (*i.e.* generation type), length of the headgroup (DPn) and nature (hydrocarbonated or fluorinated, single or double-tail) or length of the hydrophobic chains, self-assembling properties of H/F-DendriTACs are in agreement with usual trends of surfactant assemblies, *e.g.,* as a function of chain length or polar head volume. Thus, thanks to their great structural versatility, H/F-DendriTACs can provide highly tunable self-assembly morphologies that can be adapted to specific applications.

INTRODUCTION

Amphiphilic molecules are ubiquitous in everyday life as they can be found in cosmetic formulations,[1] food, pharmaceutical,[2] ink, paint, and coating industries.[3-5] Bearing both hydrophobic and hydrophilic parts, they exhibit interfacial activity and self-assemble into supramolecular structures. The features of the latter rely on numerous factors such as the nature and size of both hydrophobic and hydrophilic domains, their concentration, etc.[2, 4] Depending on the nature of their polar head, amphiphiles can be classified as ionic or nonionic, the latter being of particular interest for biomedical applications as their structure does not change with pH and as they mainly produce biocompatible particles.[6] For many years our team has been developing biocompatible amphiphiles called TAC-surfactants comprising a Tris(hydroxymethyl)aminomethane-functionalized polyACrylamide (TAC) backbone as a nonionic polar head. Synthesized in one step by free radical telomerization of the Tris(Hydroxymethyl)AcrylamidoMethane (THAM) monomer,[7, 8] TAC-surfactants have been used in a wide range of biomedical applications such as drug delivery and protein stabilization.[9, 10] The use of an aliphatic hydrocarbon (H) or a fluorinated (F) tail of variable length leads to H- and F-TAC surfactants respectively. In both cases the hydrophobic tail acts as a transfert reagent (or telogen) during the THAM telomerization, giving rise to a linear polar head, composed of a variable number of water-soluble tris(hydroxymethyl)aminomethane (TRIS)

units (see Figure 1). The so-called polyTRIS head is a linear oligomer, which is assumed to wrap around itself and be an interesting alternative to polyethylene glycol (PEG) or to sugar-based polar heads.

Although F- and H-TACs are easy to prepare at the gram scale their synthesis suffers from a growing lack of batch-to-batch reproducibility as the intended size of the polyTRIS head (average degree of polymerization (DPn)) increases. Moreover, while for the F-TAC series the DPn is precisely assessed by ^{19}F-NMR titration using an external reference,[8] for H-TAC analogues the DPn is estimated by ^{1}H-NMR by comparing the area of the signal due to the methyl group of the hydrocarbon tail with that of hydroxyl groups of TRIS units. Thereby, the longer the polyTRIS moiety the lesser accurate is the DPn estimation in that case.

In order to overcome these drawbacks (structural variability, polydispersity, DPn estimation for polyTRIS of high DPn) keeping the main advantages of F- and H-TACs (high water solubility arising from the polyTRIS polar head, biocompatibility, modular structure), we have recently developed a new class of dendritic surfactants bearing dendronized PolyTRIS oligomers of short DPn (DPn<15) as polar head groups.

Dendrimers and dendrons have drawn considerable attention because of their well-defined molecular structure resulting in unique three-dimensional architecture and small hydrodynamic radius.[11] One subclass are nonionic amphiphilic dendrons.[12, 13] This subclass has been extensively exemplified by the work of Haag et al, who developed a series of hydrogenated or fluorinated glycerol-based dendrons and studied the influence of structural features on their self-assembly.[14, 15]

In comparison with F/H-TACs, which are linear oligomers whose structural modularity is limited to the length of both polar and apolar parts, dendronization is expected to increase the surface functionalization, hence the polar head volume, due to steric hindrance at the hydrophilic surface.

Design and preparation of these new dendritic surfactants, called Dendri-TACs, have been envisioned by the grafting of dendronized polyTRIS oligomers as polar head groups to single or double-tail apolar chains using click chemistry (Scheme 1). Such a synthetic pathway should provide high structural versatility combined with a well-defined, tunable and controlled preparation. By doing so, it is possible to easily tune both their hydrophilic tree-like arms structure *i.e.* both the number and the length (number average degree of polymerization, DPn) of hydrophilic branches, and to control the structure of their hydrophobic tail (single or double-tail, fluorinated or hydrocarbon chains of variable length). The central scaffold possesses a dendritic structure with multiple branching points depending on the dendron's generation (Gn) and on the valence (2 or 3) of the repetitive unit (denoted AB_2 or AB_3 respectively, see Scheme 1) used to build the scaffold, *i.e.* 2-amino-2-methylpropane-1,3-diol (AB_2 unit) or tris(hydroxymethyl)aminomethane (AB_3 unit).

Figure 1. General structure of H/F-TAC and of Dendri-TAC surfactants

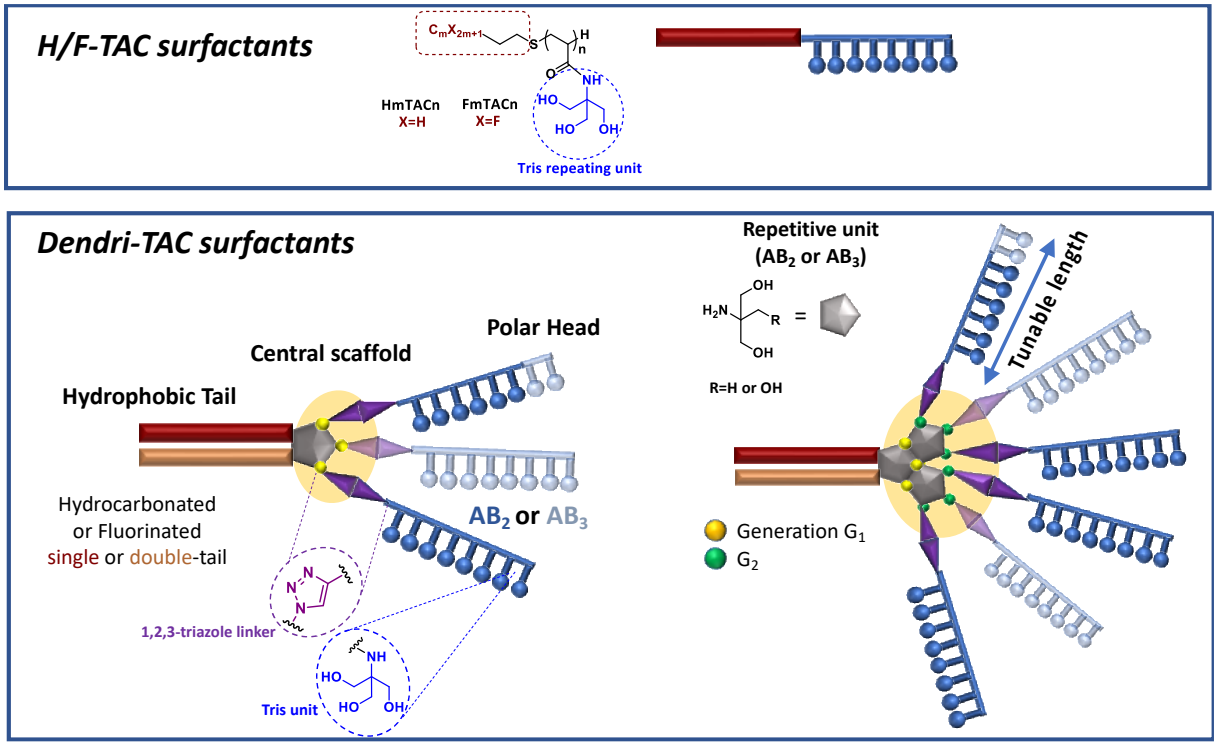

Herein, we report the synthesis of two generations of Dendri-TAC surfactants, along with the study of their structural features. AB_2 and AB_3 building blocks were used for the synthesis of G_1 Dendri-TACs, leading to either a di- or a tri-branched polar head. G_2 Dendri-TACs were synthetized using AB_2 units resulting in a tetra-cephalic polar head (See Scheme 1). The influence of structural features of the surfactant on the size and number of aggregation (N_{ag}) of resulting self-assembled architectures was studied by DLS and SAXS analyses.

RESULTS AND DISCUSSION

Synthesis. The Dendri-TAC surfactant family was built following a divergent synthetic approach starting from a bifunctional repetitive unit (starting core) endowed on one side (branching point B) with hydroxyl groups convertible to propargyl ones, in order to introduce the polar head via a copper (I) catalyzed azide-alkyne cycloaddition reaction (CuAAC), and on the other side (branching point A) an amino group graftable to the hydrophobic tail (HT).[16] Retrosynthetically, the structure of Dendri-TAC molecules can be divided in 3 fragments, including the HT, the central scaffold (made of AB_3 or AB_2 units) and the polar head. Each functional block can be varied separately, sequentially coupled and reused to easily grow the library thanks to a modular synthetic strategy (See Scheme 1). This approach allows to provide a series of structurally versatile surfactants. The synthesis is based on three key steps. First, the synthesis of the oligomeric polyTRIS polar head functionalized with an azido group. Secondly, the modular synthesis of apolar propargyl building blocks resulting from the combination of the central scaffold with the HT. Finally, the conjugation of the two former synthons through a 1,2,3-triazole junction after a Cu(I)-catalyzed azide–alkyne cycloaddition (CuAAC) reaction. For the G_1 generation, three hydrocarbonated and two fluorinated tails of different length were

introduced: C_8H_{17}, $C_{12}H_{25}$, $C_{16}H_{33}$ respectively called H_8, H_{12} and H_{16} for the hydrocarbon series, and C_6F_{13} (single-tail) or diC_6F_{13} (double-tail) respectively called F_6 and diF_6 for the fluorinated one, with either AB_2 or AB_3 starting cores. For the G_2 generation, single- (F_6) or double-tail (diF_6) fluorinated surfactants were prepared starting from a AB_2-type core.

Scheme 1. Retrosynthetic pathway of Dendri-TAC surfactants

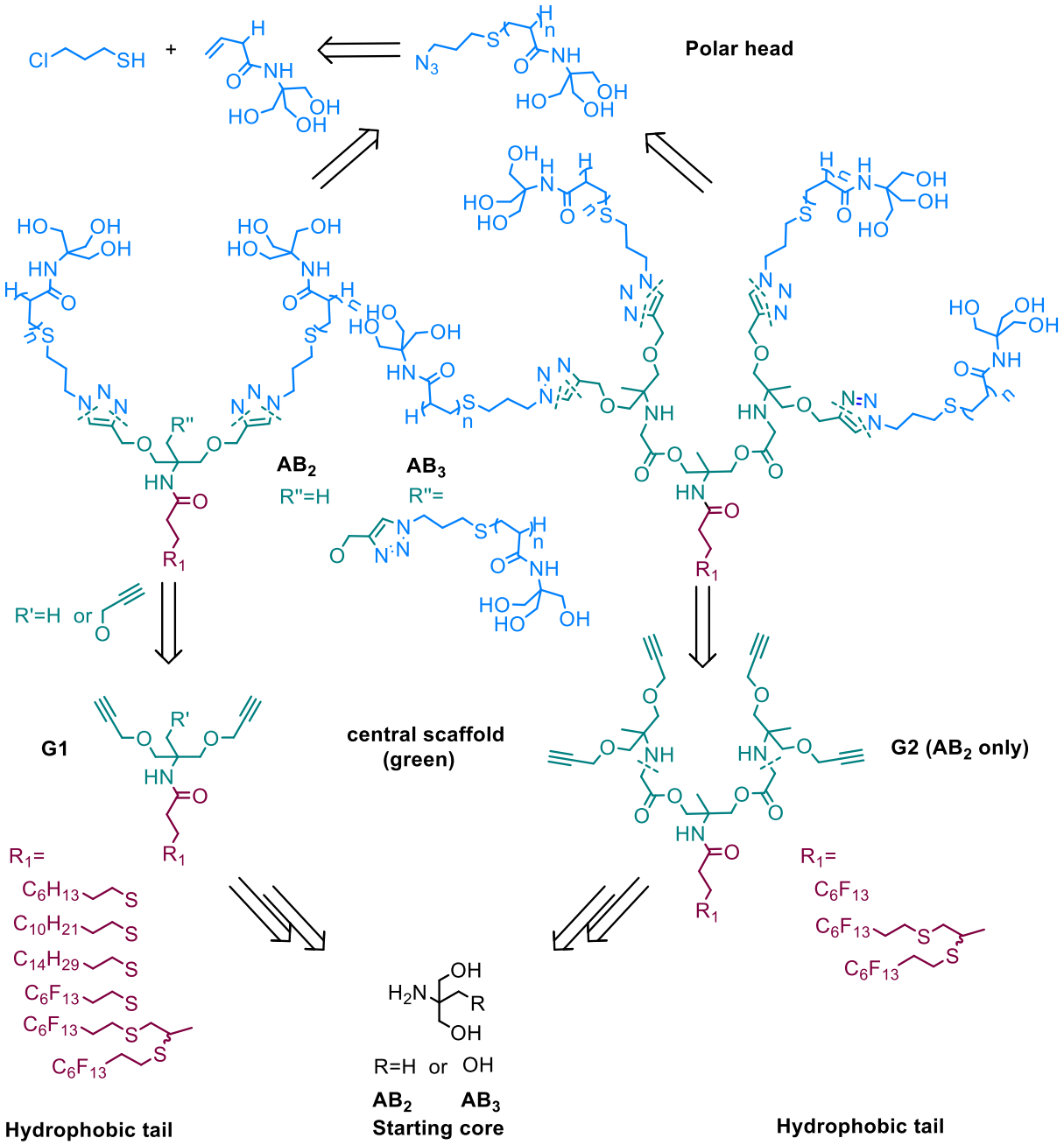

Synthesis of azido-polyTRIS. Hydrosoluble polar heads, constituted of oligomeric polyTRIS moieties functionalized with azido groups, were easily synthesized in two steps. The first step consists in a free radical telomerization of THAM monomer, performed in methanol with chloropropanethiol as transfert agent and 2,2'-azobisisobutyronitrile (AIBN) as radical initiator. Then, an azido group is introduced by nucleophilic substitution of the chlorine atom in water. According to the choice of initial monomer/telogen molar ratio ($1/R_0$), the number of n repeating TRIS units (n=DPn) can be adjusted. Two $1/R_0$ ratios were intended namely 5 and 12. After a purification step by size exclusion chromatography, the resulting DPn of azido-polyTRIS oligomers were assessed by ^{1}H-NMR, and found to be of 6 and 10 for compounds **2a** and **2b** respectively (see Scheme 2). This slight drift of the DPn values arises from the fact that free radical telomerization does not offer the same level of DPn control as living polymerization techniques. However, it is a simpler, low-cost and more straightforward synthetic methodology.[17]

Scheme 2. Synthetic pathway of azido-polyTRIS oligomers

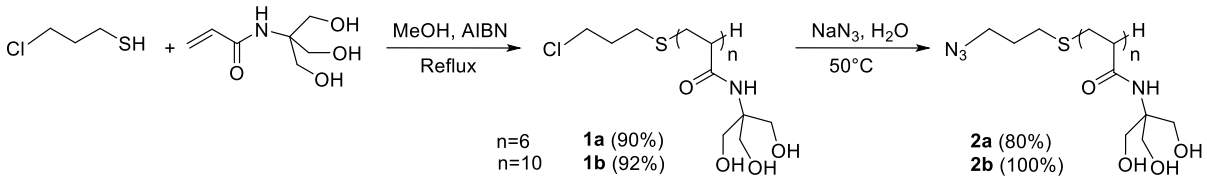

Synthesis of apolar building blocks. For all surfactants, the amino group of the AB_2 or AB_3 central scaffold is the anchor point of the HT through an amide junction. As shown in scheme **3**, for single-tail analogues the amino group of the starting material (2-amino-2-methylpropane-1,3-diol or tris(hydroxymethyl)aminomethane) was first grafted to an acryloyl moiety (compounds **3a** and **3b**) followed by the propargylation of hydroxyl groups and consecutive thiol-ene Michael addition of intermediates (compounds **4a** and **4b**) to commercially available

alkyl ($C_6H_{13}SH$, $C_{10}H_{21}SH$, $C_{14}H_{29}SH$) or fluoroalkyl thiols ($C_6F_{13}C_2H_4SH$). Apolar single tails resulting from these three steps were referred as H_8, H_{12}, H_{16} and F_6, respectively (on compounds **5 a-b** to **8 a-b**).

Scheme 3. Synthetic pathway of single-tail apolar building blocks for G_1 DendriTACs

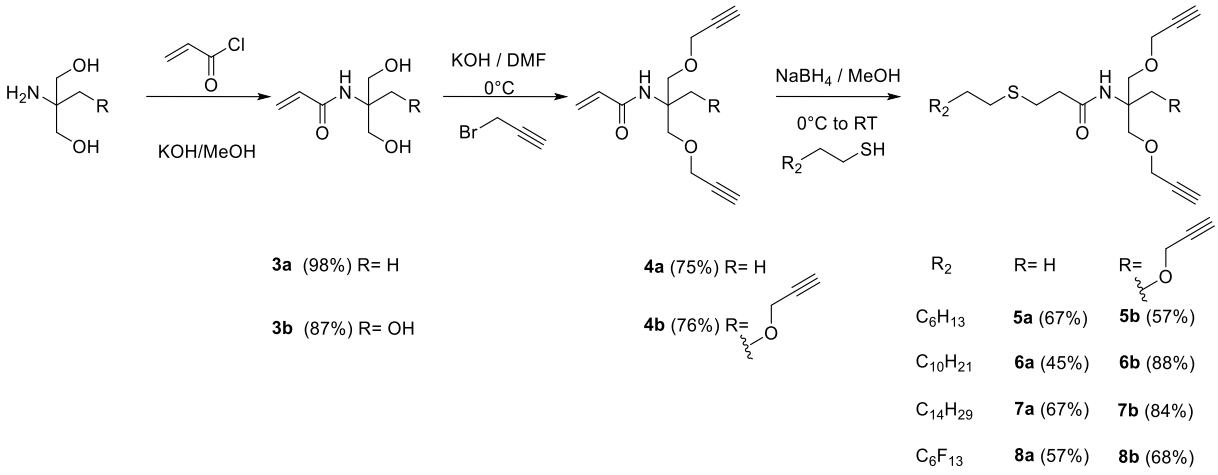

The synthesis of double-tail fluorinated surfactants (compounds **13a** and **13b**) is described in Scheme **4**. The synthesis consists in the preparation of propargyl analogues of 2-amino-2-methylpropane-1,3-diol and of tris(hydroxymethyl)aminomethane as previously described by Chabre *et al*[18] and their consecutive coupling to a double-tail acid (compound **9**) under classical conditions of peptide synthesis. The latter double-tail acid being obtained in parallel by the thiol-yne click reaction of an alkynyl carboxylic acid with an alkyl or fluoroalkyl thiol, namely 4-pentynoic acid and 2-perfluorohexylethyl thiol herein. This dihydrothiolation reaction, conducted under radical conditions using AIBN, demonstrates remarkable robustness, versatility, and compatibility with a diverse range of functional groups.[19]

Scheme 4. Synthetic pathway of double-tail apolar building blocks for G_1 DendriTACs

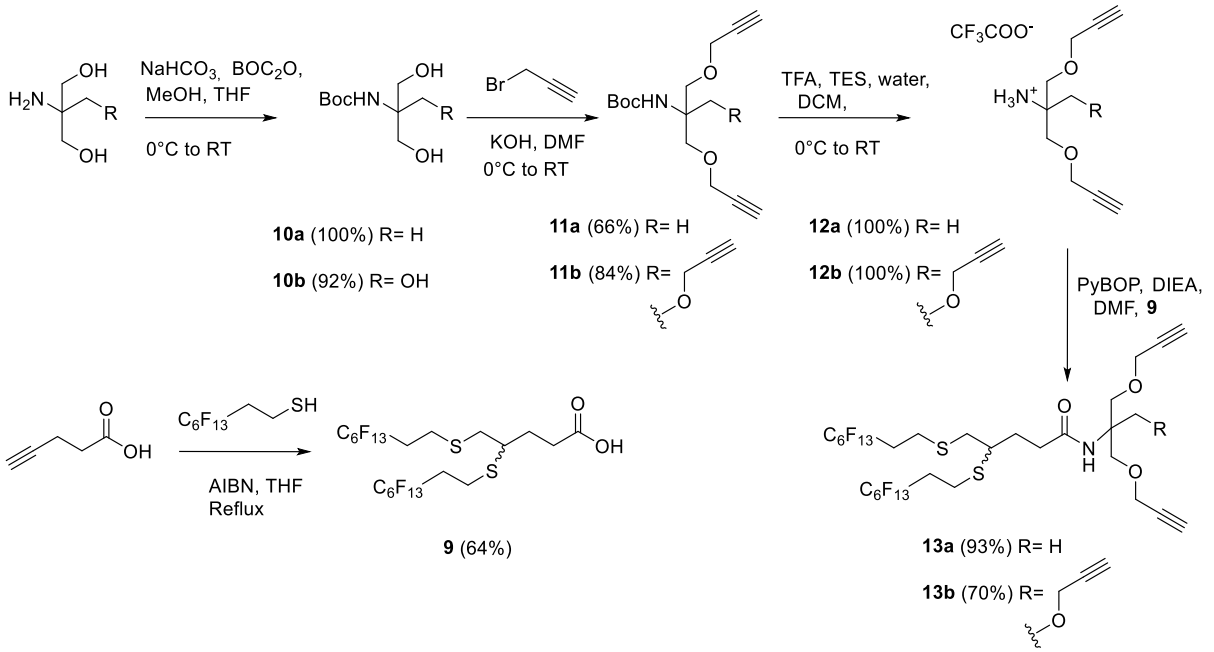

159

160 An alternative synthetic pathway for the G1 apolar building block was also followed in order
161 to prevent thiol-yne side additions and improve the overall yield. Hence, a Michael addition
162 was first performed on compounds **3a** and **3b** before the introduction of propargyl groups, as
163 shown in scheme **5**. The addition was achieved in presence of a catalytic amount of Hunig's
164 base to obtain compounds **14a** & **14b** in quantitative yield. It is noteworthy that this reaction
165 condition (methanolic N,N-Diisopropylethylamine) allowing a quantitative Michael addition
166 on **3a** and **3b** completely failed when performed on compounds **4a** and **4b**. However, lower
167 yields were obtained for the following Williamson reaction compared to the original pathway
168 described on scheme **3**, with 41 % & 54 % yield against 75% & 76% yield respectively. This
169 result may be due to the retro-Michael reaction that may have occurred under basic conditions
170 or prolonged reaction time.[20, 21] Overall yields were actually close, with 43% & 52% for the
171 original pathway against 41% & 54% for the alternative pathway.

172 **Scheme 5.** Alternative synthetic pathway of G1 apolar building blocks (single-tail)

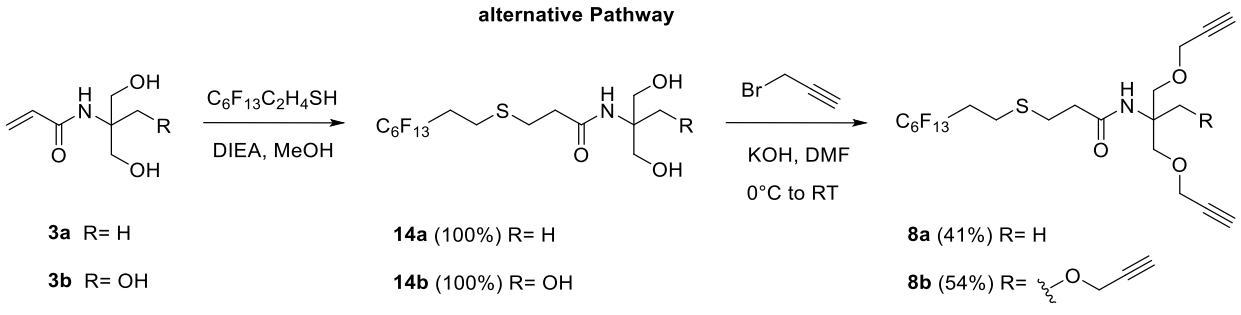

173

174

175

176 **DendriTAC second generation (G_2).** To build the apolar building blocks for the synthesis
177 of G_2 DendriTACs, an approach comprising an ester bond was applied as shown in scheme **6**
178 consisting in 3 steps. Only AB_2 repetitive units were used in order to limit steric hindrance and
179 repulsive interactions between oligomeric branches. The HT was either constituted of
180 commercially available 1H, 1H, 2H, 2H-perfluorononanoic acid or with the previously
181 synthesised fluorinated double-tail acid **9**. These HT and the AB_2 starting core were combined
182 through a peptide coupling, using EEDQ in ethanol at reflux, to obtain the diols **15a** and **15b** in
183 63% and 83% yield respectively. The second step involves the acylation of these diols with the
184 2-chloroacetyl chloride in DMF for the single-tail analogue and THF for the double-tail one, in
185 order to overcome solubility problems observed with DMF for the latter, to afford the dichloride
186 **16a** and **16b** in close yields, namely 84% and 81%. Then, compounds **16a** and **16b** underwent
187 the Finkelstein reaction to promote the nucleophilic substitution of chlorides with the di-
188 propargyl **13a** affording the G_2 apolar building blocks **17a** and **17b** in 69% and 42 % yield
189 respectively.

190 **Scheme 6.** Synthetic pathway of apolar building blocks for G_2 DendriTACs

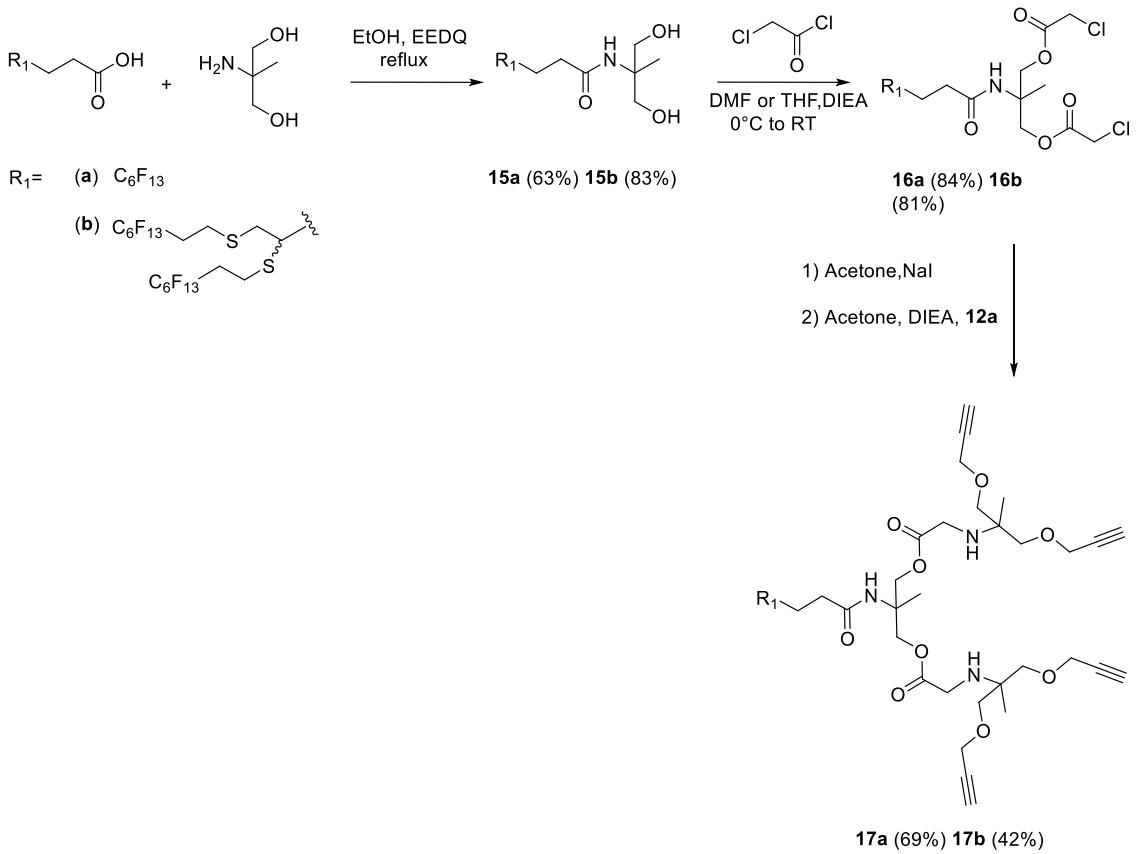

191

192

193 **Amphiphilic "click" conjugates: Coupling between the azido-polyTRIS and**
194 **propargylated apolar building blocks.** The final key step of our modular synthetic strategy
195 relied on the formation of triazole junction, employing the most widely used click method, *e.g.*
196 the Cu(I)-catalyzed azide–alkyne cycloaddition (CuAAC), to produce amphiphilic conjugates.
197 This is an attractive method for bioconjugation due to its high yields, robustness, tolerance
198 toward functional group, simple reaction conditions and generally lack of side reaction
199 occurrence.[22, 23]

200 The click reactions between apolar building blocks **5-8, 14,** and **17** and two azido-polyTRIS
201 analogues of different DPn (**2a** or **2b**) afforded the first and second generation of dendriTAC
202 surfactants **18-23** and **24,** respectively. Cycloadditions were carried out in a mixture of DMF
203 and water at 50°C, with a combination of copper (II) and sodium ascorbate as the source of
204 Cu(I) for the catalytic system. The total conversion of the alkyne to triazole was monitored by
205 ^{1}H-NMR, with the deshielding of the signal, assigned to the CH_2 in α position of the alkyne,

from δ = 4.12 ppm to δ = 4.54 ppm after the triazole formation (see Figure **2**). Both F- and H-DendriTAC surfactants were purified by size exclusion chromatography (SEC) on a Sephadex LH-20 column with MeOH as eluent. The F-DendriTAC series was consecutively purified by fluorous solid phase extraction (FSPE). The main impurity was the unreacted azido-polyTRIS. Hence, to confirm its removal during the purification process, a 2D [1H,1H] COSY NMR experiment was conducted, as signals of this unreacted azido-polyTRIS were overlapping with signals from the newly formed amphiphilic click conjugates on ^{1}H-NMR spectra. The total disappearance of cross peaks of coupled protons at δ = 1.78 ppm, ascribed to the three methylene groups of the terminal propyl chain of the azido-polyTRIS (**1a**, **2a** & **3a** in Figure **3**) was observed. As shown in Table 1, except for compound **20a**, purified DendriTACs showed a slight increase in DPn compared to starting azido-polar heads **2a** (DPn = 6) or **2b** (DPn = 10). This DPn shift can arise from the fractionation of DendriTACs, during the final LH-20 purification step. According to the Sephadex column features (column volume, packing…) the molecular size distribution of these branched molecules can be refined compared to starting linear oligomers **2a** and **2b**, thus leading to collected fractions of interest exhibiting new DPn values. It is also noteworthy that DendriTACs of low DPn and unreacted azido-polyTRIS analogues of high DPn can coelute during the size exclusion chromatography which contributes to limit some reaction yields from 20% to 70%. For the second generation, the low yields obtained might be due to the ester hydrolysis that may have occurred during the coupling or purification steps.

Figure 2. Click reaction monitoring. *Above*: example of ^{1}H-NMR spectrum of a fluorinated HT central core. *Below*: ^{1}H-NMR spectrum of a total reaction completion.

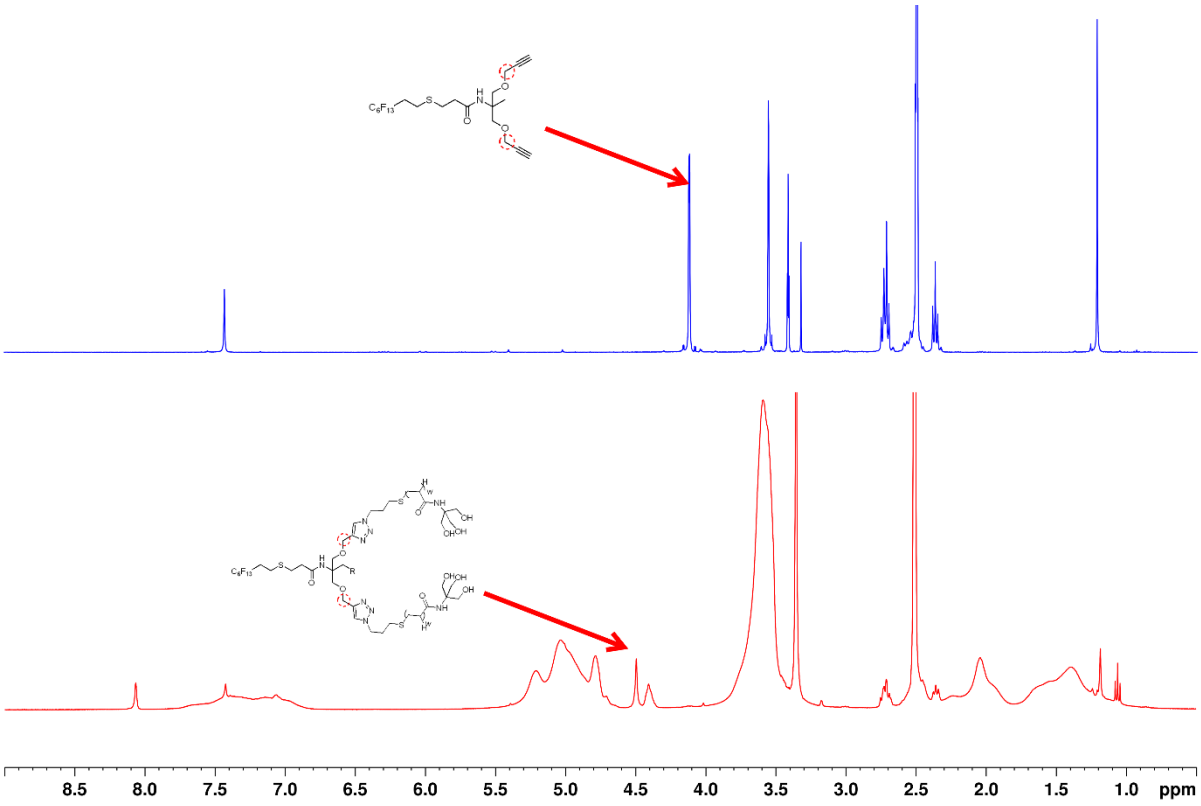

229

230 **Figure 3.** Overlay of 2D [1H,1H]-COSY NMR spectrum, in blue propargylated apolar moiety

231 spectrum and in red a DendriTAC spectrum (F_6DiTAC$_6$) after purification

232

233

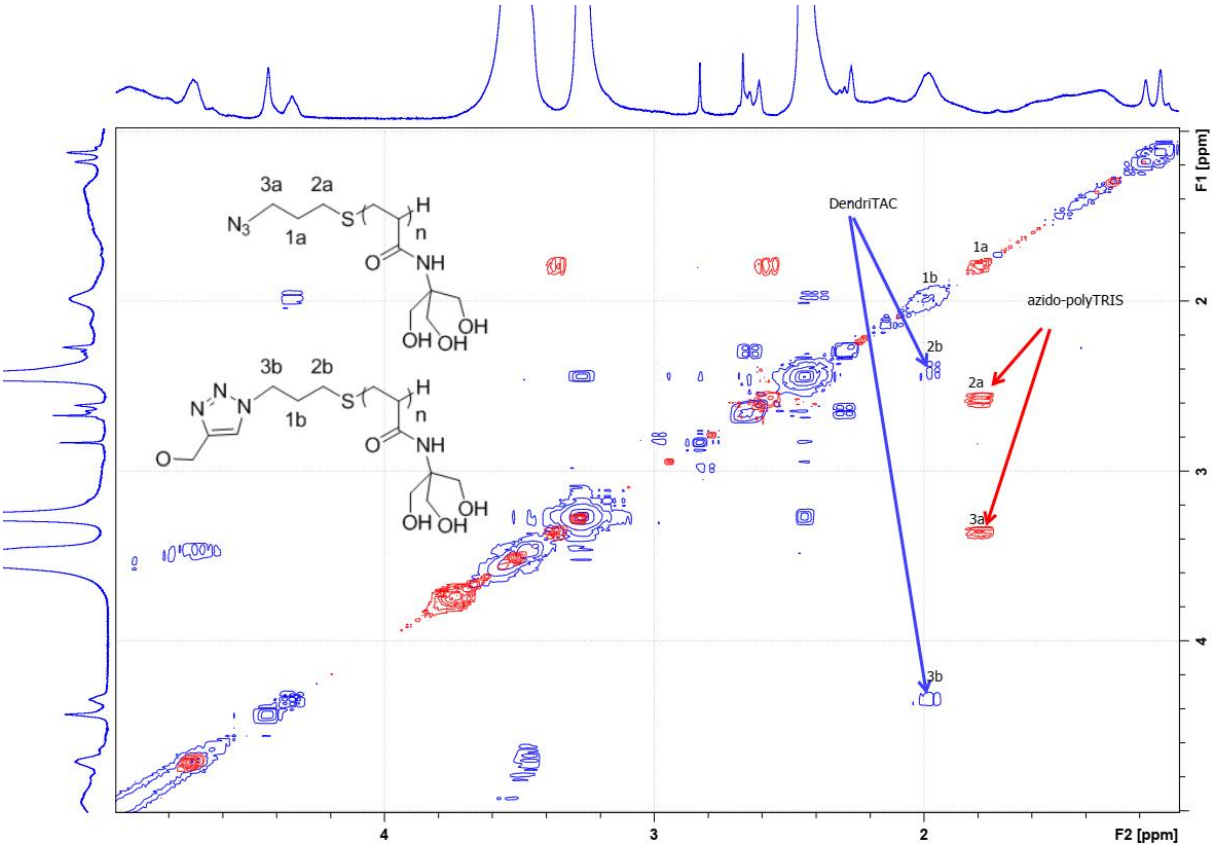

Scheme 7. Click reaction for G_1 DendriTAC surfactants' synthesis

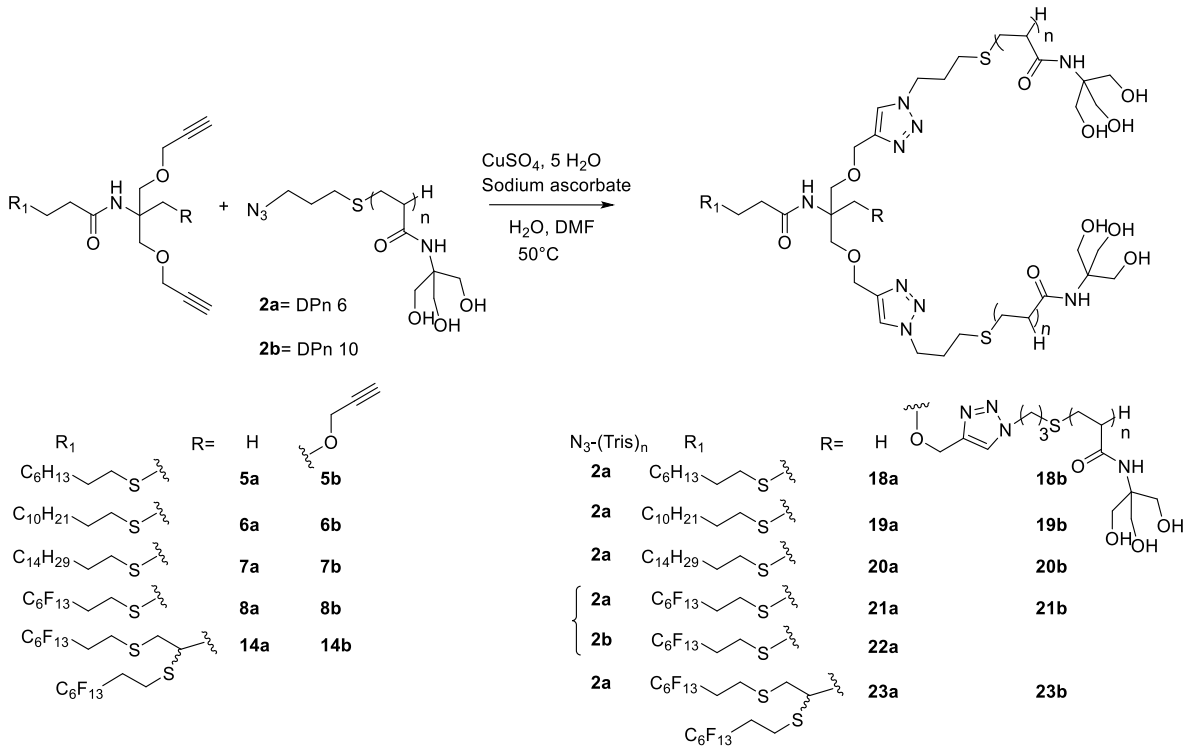

Scheme 8. Click reaction for G_2 DendriTAC surfactants' synthesis

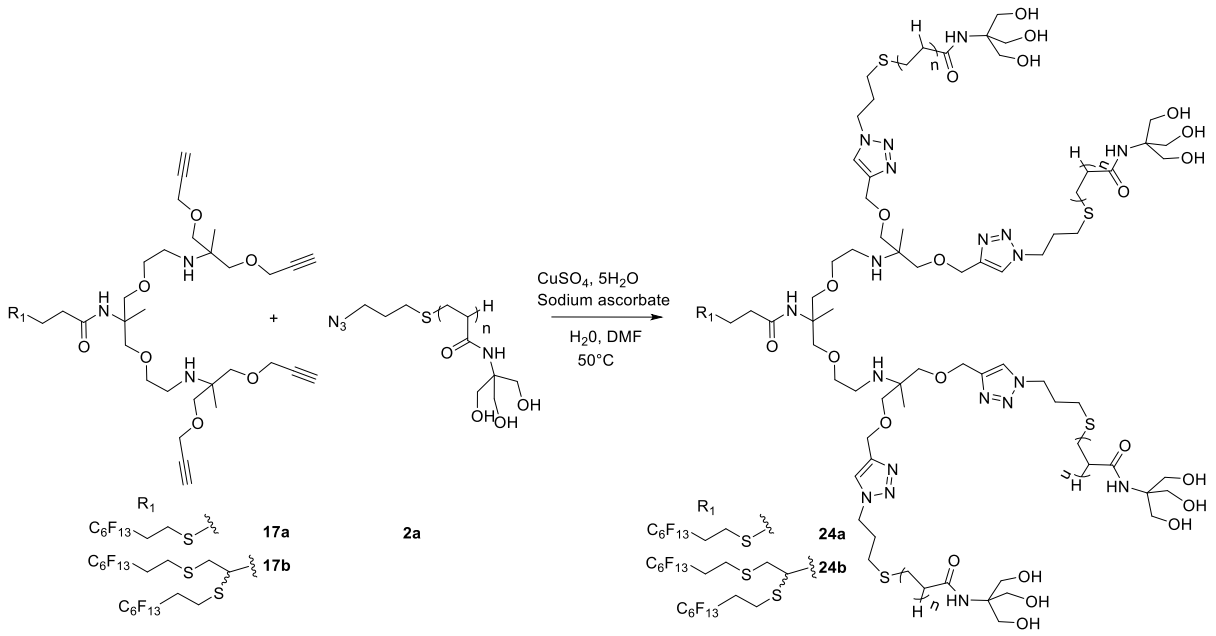

Table 1. Surfactants' synthesis summary and characterization

G	HT[1]	PH[2]	Ref	Yield[3]	DPn	Surfactant	Mn[4] (^{1}H-NMR) g/mol	Mn[5] (GPC) g/mol	$Đ_M$[6]
G_1	5a	2a	**18a**	30%	9	H_8DiTAC_9	3769	2170	1.11
G_1	6a	2a	**19a**	63%	9	$H_{12}DiTAC_9$	3824	1940	1.11
G_1	7a	2a	**20a**	22%	3	$H_{16}DiTAC_3$	1779	N/A[7]	N/A
G_1	8a	2a	**21a**	20%	7	F_6DiTAC_7	3301	2282	1.13
G_1	8a	2b	**22a**	73%	11	F_6DiTAC_{11}	4702	2094	1.13
G_1	5b	2a	**18b**	43%	6	$H_8TriTAC_6$	3939	2226	1.12
G_1	6b	2a	**19b**	41%	8	$H_{12}TriTAC_8$	5045	1919	1.14
G_1	7b	2a	**20b**	29%	8	$H_{16}TriTAC_8$	5101	1921	1.16
G_1	8b	2a	**21b**	65%	7	$F_6TriTAC_7$	3296	2420	1.11
G_1	13a	2a	**23a**	56%	6	DiF_6DiTAC_6	3357	3208	1.06
G_1	13b	2a	**23b**	80%	8	$DiF_6TriTAC_8$	4403	2290	1.17
G_2	17a	2a	**24a**	31%	6	$F_6TetraTAC_6$	5592	2582	1.09

G_2	17b	2a	**24b**	30%	6	$DiF_6TetraTAC_6$	6058	3094	1.10

[1] HT: hydrophobic tail; [2] PH: Polar head; [3] Click reaction yield; [4] Number-averaged weights in g/mol determined by ^{1}H-NMR in DMSO-d_6; [5] Number-averaged weights in g/mol determined by GPC; [6]Molar Mass Dispersities ($Đ_M$ =Mw/Mn[5]); M_n and $Đ_M$ were determined by DMF (5mM LiBr) SEC against linear polystyrene standards. [7]N/A: not applicable

DendriTAC surfactants were analyzed by ^{1}H-NMR and by gel permeation chromatography (GPC), number-averaged molecular weights (M_n) were determined by ^{1}H-NMR (M_n[4]) and by GPC (M_n[5]) while weight-averaged molecular weights (Mw) and polydispersity ($Đ_M$) were assessed by GPC only. It is noteworthy that relatively narrow $Đ_M$ values, (comprised between 1.06 and 1.17) were obtained for DendriTACs (Table 1), meaning that the synthesis of azido-polyTRIS series somehow occurred in a controlled manner.

Self-assembly studies. DLS and SAXS experiments have been performed to characterize structural parameters, in terms of size, shape, aggregation number of this new family of hydrogenated and fluorinated surfactants in aqueous solution. H/F-DendriTACs were dissolved in Milli-Q water and studied as a function of surfactant concentration between 0.8 and 50 mg/mL to highlight changes in shape and/or intermicellar weak interactions. DLS experiments were conducted prior to SAXS in order to evaluate both polydispersity (PDI) of surfactant solutions and hydrodynamic radius (R_H) of surfactant assemblies in solution. The PDI values of all compounds were found less than 0.2 suitable for SAXS experiments (see SI, Table S1). Indeed, SAXS analyses require quite monodisperse samples for reliable results. SAXS profiles are shown only at 20 or 25 mg/mL in Figure **4**. SAXS patterns with concentration were measured only for H-DendriTACs (see SI, Figure S4) due to the low quality of SAXS curves (ratio signal/noise) for F-DendriTACs at low concentrations. For all H/F-DendriTACs, the radius of gyration (R_G) was determined from the linear Guinier approximation $\mathrm{Ln}I(q) = \mathrm{Ln}I(0) - (qR_G)^2/3$ at very small angles, *i.e.* such that $qR_G < 1.3$) and the maximum micelle dimension (D_{max}) from the pair distribution function (PDF) by Inverse Fourier Transformation of the

scattering intensity using the program GNOM [24] (see SI, Figure S2A). A Kratky representation (*i.e.* a plot $q^2I(q)$ as function of q) was also performed to evaluate if the assemblies were globular, flexible or non-assembled. The aggregation number N_{ag}, *i.e.* the number of surfactant molecule per surfactant assembly, was finally determined from the absolute forward intensity, $I(0)$ in cm^{-1}, *via* the expression:

$$N_{ag} = N_a \frac{I_{surf}(0)}{M_{mono}.c[r_0.v_p.(\rho_{surf} - \rho_0)]^2}$$

with N_a the Avogadro's number, v_p the specific volume of surfactant (cm^3/g), ρ_{surf} and ρ_0 the electron scattering length densities (e^-/cm^3) of surfactant and water respectively, M_{mono} the molar mass of each surfactant monomer, r_0 the classical electron radius equal to 0.28179 10^{-12} cm/e^-. The partial specific volumes, v_p, were calculated from chemical composition.[25] All structural parameters are listed in table **2**.

Figure 4: SAXS profiles, $I(q)$ versus q, for H-DendriTAC (A) at 25 mg/mL (H_8-Di & TriTAC, H_{12}-Di & TriTAC) and 20 mg/mL (H_{16}-Di & TriTAC), for F-DendriTACs (B) at 20 mg/mL. (The curves are shifted for more clarity: ×5, ×10, ×50, ×100 represents offset parameter of the curve from its original position)

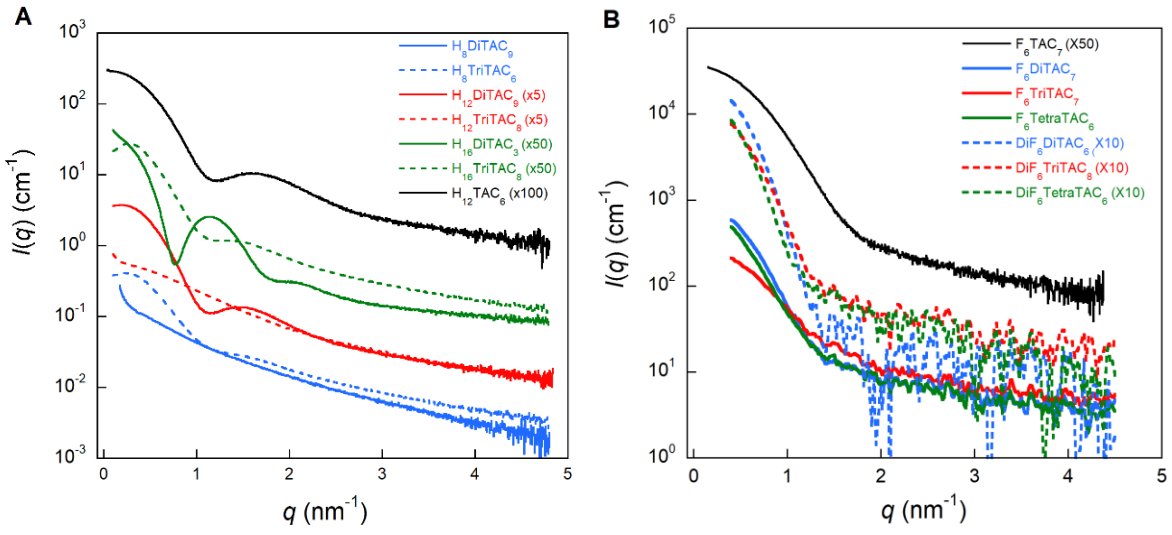

Table 2: Structural parameters of H/F-DendriTAC assemblies obtained from SAXS and DLS analysis

Entry	Surfactant	DPn	Total TRIS units	R_G nm (SAXS)	D_{max} nm (SAXS)	R_H nm (DLS)	N_{ag} (SAXS)
	H-DendriTACs†						
1	H_8DiTAC_9	9	18	2.20+/-0.05	7.5+/-0.5	1.5	3
2	$H_8TriTAC_6$	6	18	2.75+/-0.01	9.0+/-0.5	1.5	7
3	$H_{12}DiTAC_9$	9	18	3.05+/-0.01	8.7+/-0.3	3.5	20
4	$H_{12}TriTAC_8$	8	24	1.79+/-0.01	6.5+/-0.1	4.5	1
5	$H_{16}DiTAC_3$	3	6	4.19+/-0.01	10.4+/-0.1	5.2	21
6	$H_{16}TriTAC_8$	8	24	3.25+/-0.05	9.5+/-0.1	2.8	15
	F-DendriTACs‡						
7	F_6DiTAC_7	7	14	2.80+/-0.05	7.6+/-0.1	2.4	14
8	F_6DiTAC_{11}	11	22	3.10+/-0.05	9.9+/-0.1	3.3	9
9	$F_6TriTAC_7$	7	21	2.37+/-0.02	6.6+/-0.1	1.7	3
10	$F_6TetraTAC_6$	6	24	2.72+/-0.02	7.0+/-0.1	2.8	7
11	DiF_6DiTAC_6	6	12	3.50+/-0.05	9.5+/-0.5	4.6	37
12	$DiF_6TriTAC_8$	8	24	2.75+/-0.12	8.05+/-0.1	1.2	11
13	$DiF_6TetraTAC_6$	6	24	3.63+/-0.02	9.3+/-0.5	4.7	15
	H/F-TACs†						
14	$H_{12}TAC_6$	6	6	2.78+/-0.01	8.5+/-0.3	3.0	29
15	F_6TAC_7	7	7	2.37+/-0.01	7.7+/-0.1	2.5	13

*Structural parameters for H/F-DendriTACs and H/F-TACs at 20-25 mg/mL; †these SAXS measurements were performed in a q-range of 0.032–4.93 nm^{-1} on BM29 at ESRF; repulsive interactions at very small angles are clearly visible for some assemblies (entries **2**, **3**, **6**). ‡ These SAXS measurements were performed in a q-range of 0.2– 4.5 nm^{-1} on a bench-top SAXS system at ICSM; no specific interactions are visible in this q-range.*

From scattering experiments (Figure **4**) we observe that H/F-DendriTACs form small globular assemblies in water regardless of their tree-like structure (*i.e.* generation type), length of the headgroup (DPn) and nature (hydrocarbonated or fluorinated, single or double-tail) or length of the hydrophobic chains. This is confirmed by the Kratky plots (See SI Figures S2B-C), which highlight a globular micellar structure as seen by a bell-shaped (Gaussian) peak for all H/F-DendriTACs at small q (< 1 nm^{-1}), except for $H_{12}TriTAC_8$ and H_8DiTAC_9, which show a plateau at large q typical of non-globular or flexible objects. Some SAXS curves (for surfactants $H_{12}TAC_6$, $H_{12}DiTAC_9$ and $H_{16}DiTAC_3$ in Figure **4**A) exhibit a distinct 2^{nd} maximum in the intermediate *q*-region, whose value is inversely proportional to a size in the micelle. This peak, which is characteristic of a core-shell structure where a large difference in the scattering contrast exists between the polar head group and the apolar tail, is more pronounced for H-DendriTACs than for F-DendriTACs. In addition, regarding surfactants $H_8TriTAC_6$, $H_{12}DiTAC_9$ and $H_{16}TriTAC_8$, the profile of scattering intensities recorded at small angles (*i.e.* low *q*-region) is clearly indicative of repulsive interactions between micelles (Figure **4**/A). In table **2** are listed R_H, the micelle volume-weighted hydrodynamic radius determined by DLS, R_G the radius of gyration and D_{max}, the maximum dimension of the DendriTAC assemblies, both determined by SAXS. For all surfactants, R_H and R_G are lower than 6 nm, and D_{max} remains below 11 nm. Compared to conventional surfactants,[26] all compounds present small aggregation numbers, except DendriTAC **4** ($H_{12}TriTAC_8$), which is a monomer form at this concentration in view of its low aggregation number (N_{ag} =1). Overall, self-assembling properties are in agreement with usual trends of surfactant assemblies, *e.g.,* as a function of chain length or polar head volume. However, the high degree of structural versatility of H/F-DendriTACs, which offers a wide range of aggregate morphologies, can be tailored to specific applications.

Regarding H-DendriTACs, for a defined headgroup, *i.e.* same length and tree-like structure (*e.g.* entries **1** & **3** and **4** & **6**), N_{ag}, R_G and almost all R_H values increase with the elongation of

the hydrophobic tail reflecting a better anchoring of monomers in the micelle due to higher hydrophobic interactions between apolar chains, consistent with literature and previous studies.[27, 28] The aggregation numbers approximatively increase by 15 monomers per micellar aggregates for a group of four carbons added on the hydrocarbonated tail. Whereas for the same tree-like structure, this extension of the hydrophobic tail (four carbons) is balanced by a reduction in the length of the headgroup, *i.e.* DPn values, and leads to an equivalent aggregation number (entries **3** & **5**). For the same apolar chain, the micelle size decreases with increasing total number of TRIS units (entries **3** & **4** and **5** & **6**), which is achieved by adding a polar branch from AB_2 to AB_3 with either comparable (entries **3** & **4**) or higher DPn values (entries **5** & **6**). This is in agreement with the concept of molecular packing parameter *P* (*P* being defined as $V_o/a_e l_o$, where V_o is the surfactant tail volume, l_o is the tail length, and a_e is the equilibrium area per molecule at the aggregate surface) introduced by Israelachvili et al. [29] The addition of several hydrated TRIS units (either by elongation or branching enhancement) improves the repulsion between polyTRIS branches, leading to an increase in the polar head volume and therefore in the equilibrium area a_e. This induces a decrease in the packing parameter *P* leading to the formation of smaller objects. These repulsive interactions between TRIS units at the surface of surfactants also contribute to repulsive interactions between micelles clearly observable on SAXS curves in the case of H_8TriTAC$_6$, H_{12}DiTAC$_9$ and H_{16}TriTAC$_8$ (entries **2**, **3**, **6**) at very small angles (*i.e.* q→0) by a decrease in $I(q)$, which can slightly underestimate R_G and forward intensity $I(0)$ thus impacting assembly size and mass values. It is noteworthy that for surfactants with both identical apolar chain length and same total number of TRIS units, micelle size decreases with longer polyTRIS branches (entries **1** & **2**), the equilibrium area a_e due to repulsion between longer AB_2-connected branches being higher than for shorter AB_3 ones.

In the case of fluorinated surfactants, the latter repulsion is counterbalanced by an improved hydrophobic interaction between fluorinated chains, also referred as “fluorophilicity”, consistent with a closely-packed fluorinated core. [30,31] This leads to a decrease of the aggregation number (entries **8** & **9**). If we compare the evolution of the structural parameters from H_8DiTAC$_9$ to H_8TriTAC$_6$ (entries **1** & **2**) with those of fluorinated surfactants with the same carbon atoms number on the hydrophobic tail, namely from F_6DiTAC$_{11}$ to F_6TriTAC$_7$ (entries **8** & **9**), the trend between size and aggregation number is clearly reversed: for H_8-DendriTACs (entries **1** & **2**) it seems that the repulsion between the polar heads (due to a combination of steric hindrance and strong hydration of hydroxyl groups) increases with the length of the polyTRIS chains and with the easier unfolding of these chains from AB_3 to AB_2 branching type. Then, from H_8TriTAC$_6$ to H_8DiTAC$_9$ (entries **2** & **1**) the aggregation number decreases and the size of micelles too. While for F_6-DendriTACs, both hydrophobicity and lipophobicity of fluorinated chains, along with their lower conformational freedom (rigid rod-like chains) concur to a “super” hydrophobic binding interaction between F-chains (mainly driven by the entropic gain of water molecules in bulk water) and contribute to their ordered packing into the micelle core.[30-32] Their combination to bulky oligomeric head groups, probably confers a more conical shape to F-DendriTAC monomers with a more "classical" influence of the tree-like structure on the volume of the heads: AB_3 induces a greater curvature of the surfactant with stronger anchoring of fluorinated tails in the micelle core, resulting in smaller micelles when moving from AB_2 to AB_3. The general trend observed from F_6DiTAC$_{11}$ to F_6TriTAC$_7$ (entries **8** & **9**) is that both the aggregation number and the micelle size decrease even though the AB_2 analogue F_6DiTAC$_{11}$ is endowed with longer polyTRIS branches. It is interesting to note that for an equivalent total number of TRIS units (18 for the two H_8-DendriTACs and 21-22 for the two F_6-DendriTACs), the impact of the “branching/elongation” effect is reversed between H_8- and F_6- chains. The aggregation behavior of F-DendriTACs

seems to be more affected by the branched geometry of the polar head groups (R_G-R_H and N_{ag} decrease with the branching effect) compared to H-DendriTACs more affected by the elongation of polyTRIS units (R_G-R_H and N_{ag} decrease with the elongation effect).

Figure 5: A, B, C represent respectively the structure (below) and proposed aggregation model (above) for G_1/AB_2, $G_1/AB3$, and $G2/AB_2$-AB_2 amphiphiles

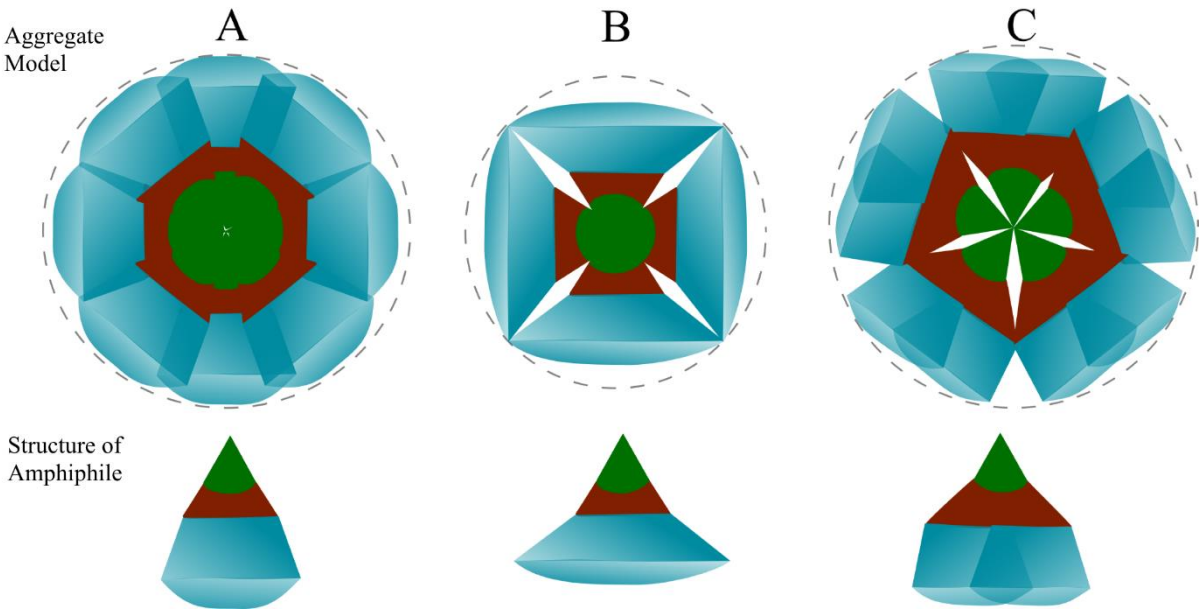

In regards to the F-DendriTACs series, they all possess the same $C_6F_{13}C_2H_4$ hydrophobic chain length, either in a single or double-tail form. Always in agreement with the concept of packing parameter, for F-DendriTACs with rather identical heads in terms of the length and number of polyTRIS branches (comparing F_6**DiTAC$_7$** to DiF_6**DiTAC$_6$**; F_6**TriTAC$_7$** to DiF_6**TriTAC$_8$** and F_6**TetraTAC$_6$** to DiF_6**TetraTAC$_6$**), as the volume of the hydrophobic part increases (from single to double-tailed surfactants), *P* increases leading to larger objects (entries **7** & **11**; **9** & **12**; **10** & **13**). In the same way, as for H-DendriTACs, the micelle size decreases with the addition of one polar branch, from AB_2 to AB_3 when polyTRIS branches have similar DPn values (entries **7** & **9**; **11** & **12**, Figure 5-A&B).

In contrast, for a same hydrophobic tail and same branching structure, when the length of the headgroup increases from 7 to 11 TRIS units per branch (entries **7** & **8**), both R_H and R_G slightly increases, whereas N_{ag} decreases. The decrease in N_{ag} can be explained by the fact that if the

388 headgroups are larger, less surfactants are required to fill the same volume. Indeed, N_{ag} is related
389 to the geometric parameters of surfactants by the expression $N_{ag} \sim (4\pi lo^2)/a_e$ (with a_e the
390 equilibrium area per molecule at the aggregate surface and lo the tail length). [33-35] Thus, if a_e
391 increases, N_{ag} decreases. However, we cannot rule out the possibility that the shape of micelles
392 has changed as a result of the concept of molecular parameter (*vide supra*). Regarding the
393 generations G_1 and G_2, for F-DendriTACs with a same AB_2 branching structure and close DPn
394 value per polyTRIS branch, F_6DiTAC$_7$ *versus* F_6TetraTAC$_6$ and DiF_6DiTAC$_6$ *versus*
395 DiF_6TetraTAC$_6$, little variation in the size of the assemblies is observed (R_G and R_H) although
396 for the single-tailed (entries **7** & **10**) R_H slightly increases, while N_{ag} is divided by at least 2 (see
397 entries **7** & **10**, **11** & **13**). This trend is consistent with the results described previously on the
398 impact of the headgroup volume. Thus, between G_1 and G_2 series with identical apolar chains,
399 the micelle shape is retained while G_2 ones have a lower N_{ag} due to the wider/bulkier headgroup.
400 Although there is no great variation in the size of the resulting assemblies, a difference in the
401 transport properties may arise from G_1 to G_2 DendriTACs due to the volume variation of the
402 central scaffold between polyTRIS branches (Figure 5-A&C).
403 For each single- or double-tail F-DendriTACs series of generation G_1, it is again noteworthy
404 that the addition of a polyTRIS branch of similar length (entries **7** & **9**, **11** & **12**) leads to a
405 decrease in micelle size. A decrease of the aggregation number is also observed as a
406 consequence of the high curvature of the polar head group of each monomer engaged in the
407 micelle.
408 **Comparison between H/F-surfactants**. It has long been shown for surfactants whose
409 hydrophobic tail contains more than 6 perfluorinated carbons linked to a short hydrocarbonated
410 part (methylene groups), that 1 CF_2 ≈ 1.5-1.7 CH_2 ref.[36, 37] This means that a F_6-chain is
411 equivalent to roughly a H_{10} one. In our case, since each perfluorocarbon tail is followed by two
412 methylene units, the tail of the F_6-chain series is therefore equivalent to that of the H_{12}-chain

413 series, as confirmed by the size parameters for H- and F-DendriTACs, which have similar DPn
414 values and same AB_2 branching type (see entries **3** & **7**). However, smaller assemblies are
415 observed with fluorinated analogues due to the enhanced hydrophobic interaction and stiffness
416 of the fluorocarbon chains that confers them a different packing into the micelle core compared
417 to their hydrocarbon analogues. This is also observed for surfactants endowed with linear polar
418 heads H- and F-TAC surfactants (see entries **14** & **15**). In both linear or dendritic families, N_{ag}
419 is lower for F_6-series than for H_{12}-series due to the bulkiest and rigidity of F-chains that do not
420 allow as much hydrophobic chains in the micelle core as for H-chains.
421 **Comparison between H/F-TAC and H/F-DendriTAC surfactants**. As mentioned above,
422 $H_{12}TAC_6$ and F_6TAC_7 can be considered to have both comparable hydrophobic contribution of
423 their tail and length of their polyTRIS polar head. However, smaller assemblies are obtained
424 for F_6TAC_7 due to the different molecular packing of fluorinated monomers into the
425 supramolecular construct. Now, if we compare the linear surfactant F_6TAC_7 to its closest
426 dendritic counterpart F_6DiTAC_7 it appears that the structural parameters of the resulting
427 assemblies (R_G, R_H and N_{ag}) are very close. Then, if we extrapolate the comparison and consider
428 F_6TAC_7 as the AB_1 analogue of the F_6-DendriTAC series, it seems that the presence of the
429 central scaffold between the F_6-chain and the polyTRIS head groups attenuates the impact of
430 the branching effect on the micelle size and aggregation number when comparing F_6TAC_7 (AB_1
431 analogue) to F_6DiTAC_7 (AB_2 analogue). However, one can assume that the presence of the two
432 triazole rings and the space between the two oligomeric head groups will influence their
433 respective performances in terms of encapsulation efficiency or as potential nanoreactors.
434 Addition of one supplementary polyTRIS branch to the polar head (from F_6DiTAC_7 to
435 $F_6TriTAC_7$) induces a decrease in the micelle size and aggregation number, as already
436 commented (entries **7** & **9**). The same tendency is observed for double-tail analogues
437 DiF_6DiTAC_6 and $DiF_6TriTAC_8$ (entries **11** & **12**). Surprisingly, the introduction of a fourth

polyTRIS branch *via* an increase in surfactant generation (from a G_1/AB_2 polar head (entry **7**) to a G_1/AB_3 (entry **9**) and then to a G_2/AB_2-AB_2 *i.e.* a TetraTAC polar head (entry **10**)) cancels out micelle size fluctuations without compensating for N_{ag} variations when moving from G_1/AB_2 to G_1/AB_3 and then to G_2/AB_2-AB_2 monomers. The same trend can be seen with the double-tail surfactants (entries **11**, **12** and **13**, Figure 5-A, B & C). Again, we can assume that for comparable object size, these different types of assemblies will not offer the same loading capacity for drug delivery or as nanoreactors. For these application types, the high intrinsic variability of the self-assemblies generated by our new family of dendritic surfactants should make H/F-DendriTACs much more versatile platforms than H/F-TACs.

CONCLUSION

In this study, the synthesis of a new dendritic surfactant family called H/F-DendriTAC is described, consisting of either hydrogenated or fluorinated alkyl chains grafted to dendronized hydrophilic oligomers leading to a high structural modularity. All compounds showed a good solubility in water, which allowed their self-assembling study. The aggregation behavior of fifteen surfactants was investigated using small-angle X-ray scattering (SAXS) and dynamic light scattering (DLS) to assess micellar structural parameters, such as their radius of gyration (R_G), volume-weighted hydrodynamic radius (R_H) and aggregation number (N_{ag}). The versatility of the resulting molecular architectures (varying in both the nature, length and number of hydrophobic chains, and number and length of oligomeric polyTRIS polar branches) allows to obtain a large library of micellar aggregates of nanometric size and variable aggregation number. Overall, the high structural versatility of H/F-DendriTAC surfactants, which offers tunable self-assembly behaviors, opens perspectives for a wide range of applications. In ongoing researches, their potential use as nanoreactors for micellar catalysis and as nanocarriers for drug delivery will be investigated.

Acknowledgements

This research was funded by ERANET EuroNanoMed-II program (Project SonoTherag). The authors are grateful to the LaBex ChemiSyst for funding the PhD thesis grant of V. Lacanau (ANR-10-LABX-05-01). We gratefully acknowledge ESRF (European Synchrotron Radiation Facilities at Grenoble, France) for beamtimes on BM29 beamline, and we thank Dr Petra Pernot (BM29) for assistance during SAXS experiments. We also thank Dr Olivier Diat from ICSM (Marcoule-France) for giving us access to the ICSM SAXS instrument during the ESRF shutdown for experiments on F-DendriTACs and his help for SAXS measurements.

REFERENCES

(1) Yukuyama, M. N.; Ghisleni, D. D. M.; Pinto, T. J. A.; Bou-Chacra, N. A. Nanoemulsion: process selection and application in cosmetics - a review. *Int. J. Cosmetic Sci.* **2016**, *38* (1), 13-24. DOI: 10.1111/ics.12260.

(2) Sorrenti, A.; Illa, O.; Ortuno, R. M. Amphiphiles in aqueous solution: well beyond a soap bubble. *Chem. Soc. Rev.* **2013**, *42* (21), 8200-8219. DOI: 10.1039/c3cs60151j.

(3) Schramm, L.; Stasiuk, E.; Marangoni, G. Surfactants and their Applications. *Annu. Rep. Prog. Chem., Sect. C: Phys. Chem.* **2003**, *99*, 3-48. DOI: 10.1039/B208499F.

(4) Malmsten, M. *Surfactants and polymers in drug delivery*; 2002.

(5) Tadros, T. Food Surfactants. In *Encyclopedia of Colloid and Interface Science*, Tadros, T. Ed.; Springer Berlin Heidelberg, 2013; pp 555-556.

(6) Parshad, B.; Prasad, S.; Bhatia, S.; Mittal, A.; Pan, Y.; Mishra, P. K.; Sharma, S. K.; Fruk, L. Non-ionic small amphiphile based nanostructures for biomedical applications. *RSC Adv.* **2020**, *10* (69), 42098-42115. DOI: 10.1039/D0RA08092F.

(7) Desgranges, S.; Lorton, O.; Gui-Levy, L.; Guillemin, P.; Celicanin, Z.; Hyacinthe, J. N.; Breguet, R.; Crowe, L. A.; Becker, C. D.; Soulie, M.; et al. Micron-sized PFOB liquid core droplets stabilized with tailored-made perfluorinated surfactants as a new class of endovascular sono-sensitizers for focused ultrasound thermotherapy. *J. Mater. Chem. B* **2019**, *7* (6), 927-939. DOI: 10.1039/c8tb01491d.

(8) Astafyeva, K.; Somaglino, L.; Desgranges, S.; Berti, R.; Patinote, C.; Langevin, D.; Lazeyras, F.; Salomir, R.; Polidori, A.; Contino-Pepin, C.; et al. Perfluorocarbon nanodroplets stabilized by fluorinated surfactants: characterization and potentiality as theranostic agents. *J. Mater. Chem. B* **2015**, *3* (14), 2892-2907. DOI: 10.1039/c4tb01578a.

(9) Contino-Pépin, C.; Parat, A.; Patinote, C.; Roscoe, W. A.; Karlik, S. J.; Pucci, B. Thalidomide Derivatives for the Treatment of Neuroinflammation. *ChemMedChem* **2010**, *5* (12), 2057-2064. DOI: 10.1002/cmdc.201000326.

(10) Jasseron, S.; Contino-Pépin, C.; Maurizis, J. C.; Rapp, M.; Pucci, B. In vitro and in vivo evaluations of THAM derived telomers bearing RGD and Ara-C for tumour neovasculature targeting. *Eur. J. Med. Chem.* **2003**, *38* (9), 825-836. DOI: 10.1016/S0223-5234(03)00150-8.

(11) Rosen, B. M.; Wilson, C. J.; Wilson, D. A.; Peterca, M.; Imam, M. R.; Percec, V. Dendron-Mediated Self-Assembly, Disassembly, and Self-Organization of Complex Systems. *Chem. Rev.* **2009**, *109* (11), 6275-6540. DOI: 10.1021/cr900157q.

(12) Apartsin, E.; Caminade, A.-M. Supramolecular Self-Associations of Amphiphilic Dendrons and Their Properties. *Chem. Eur. J.* **2021**, *27* (72), 17976-17998. DOI: 10.1002/chem.202102589.
(13) Thota, B. N. S.; Urner, L. H.; Haag, R. Supramolecular Architectures of Dendritic Amphiphiles in Water. *Chem. Rev.* **2016**, *116* (4), 2079-2102. DOI: 10.1021/acs.chemrev.5b00417.
(14) Singh, A. K.; Thota, B. N. S.; Schade, B.; Achazi, K.; Khan, A.; Böttcher, C.; Sharma, S. K.; Haag, R. Aggregation Behavior of Non-ionic Twinned Amphiphiles and Their Application as Biomedical Nanocarriers. *Chem Asian J* **2017**, *12* (14), 1796-1806. DOI: 10.1002/asia.201700450.
(15) Rashmi, R.; Hasheminejad, H.; Herziger, S.; Mirzaalipour, A.; Singh, A. K.; Netz, R. R.; Böttcher, C.; Makki, H.; Sharma, S. K.; Haag, R. Supramolecular Engineering of Alkylated, Fluorinated, and Mixed Amphiphiles. *Macromol Rapid Commun* **2022**, *43* (8), 2100914. DOI: 10.1002/marc.202100914.
(16) Roy, R.; Shiao, T. C. Glyconanosynthons as powerful scaffolds and building blocks for the rapid construction of multifaceted, dense and chiral dendrimers. *Chem. Soc. Rev.* **2015**, *44* (12), 3924-3941. DOI: 10.1039/c4cs00359d.
(17) Teulère, C.; Nicolaÿ, R. Synthesis of molecular brushes by telomerization. *Polym. Chem.* **2017**, *8* (34), 5220-5227. DOI: 10.1039/c7py00875a.
(18) Chabre, Y. M.; Contino-Pépin, C.; Placide, V.; Shiao, T. C.; Roy, R. Expeditive Synthesis of Glycodendrimer Scaffolds Based on Versatile TRIS and Mannoside Derivatives. *J. Org. Chem.* **2008**, *73* (14), 5602-5605. DOI: 10.1021/jo8008935.
(19) Li, L.; Zahner, D.; Su, Y.; Gruen, C.; Davidson, G.; Levkin, P. A. A biomimetic lipid library for gene delivery through thiol-yne click chemistry. *Biomaterials* **2012**, *33* (32), 8160-8166. DOI: 10.1016/j.biomaterials.2012.07.044.
(20) Berne, D.; Ladmiral, V.; Leclerc, E.; Caillol, S. Thia-Michael Reaction: The Route to Promising Covalent Adaptable Networks. *Polymers* **2022**, *14* (20). DOI: 10.3390/polym14204457 From NLM.
(21) Boncel, S.; Mączka, M.; Walczak, K. Z. Michael versus retro-Michael reaction in the regioselective synthesis of N-1 and N-3 uracil adducts. *Tetrahedron* **2010**, *66* (43), 8450-8457. DOI: 10.1016/j.tet.2010.08.059.
(22) Rostovtsev, V. V.; Green, L. G.; Fokin, V. V.; Sharpless, K. B. A Stepwise Huisgen Cycloaddition Process: Copper(I)-Catalyzed Regioselective "Ligation" of Azides and Terminal Alkynes. *Angew. Chem. Int. Ed.* **2002**, *41* (14), 2596-2599. DOI: 10.1002/1521-3773.
(23) Tornøe, C. W.; Christensen, C.; Meldal, M. Peptidotriazoles on Solid Phase: [1,2,3]-Triazoles by Regiospecific Copper(I)-Catalyzed 1,3-Dipolar Cycloadditions of Terminal Alkynes to Azides. *J. Org. Chem.* **2002**, *67* (9), 3057-3064. DOI: 10.1021/jo011148j.
(24) Svergun, D. I. Determination of the regularization parameter in indirect-transform methods using perceptual criteria. *J Appl Crystallogr* **1992**, *25* (4), 495-503. DOI: 10.1107/S0021889892001663.
(25) Durchschlag, H.; Zipper, P. Calculation of Partial Specific Volumes and Other Volumetric of Detergents and Lipids. *Jorn. Com. Esp. Deterg.* **1995**, *29*, 275-292.
(26) Linke, D. Chapter 34 Detergents: An Overview. In *Methods in Enzymology*, Burgess, R. R., Deutscher, M. P. Eds.; Vol. 463; Academic Press, 2009; pp 603-617.
(27) Oliver, R. C.; Lipfert, J.; Fox, D. A.; Lo, R. H.; Doniach, S.; Columbus, L. Dependence of Micelle Size and Shape on Detergent Alkyl Chain Length and Head Group. *PLoS One* **2013**, *8* (5), e62488. DOI: 10.1371/journal.pone.0062488.
(28) Lipfert, J.; Columbus, L.; Chu, V. B.; Lesley, S. A.; Doniach, S. Size and Shape of Detergent Micelles Determined by Small-Angle X-ray Scattering. *J. Phys. Chem. B* **2007**, *111* (43), 12427-12438. DOI: 10.1021/jp073016l.
(29) Israelachvili, J. N.; Mitchell, D. J.; Ninham, B. W. Theory of self-assembly of hydrocarbon amphiphiles into micelles and bilayers. *J. Chem. Soc., Faraday Trans. 2* **1976**, *72* (0), 1525-1568. DOI: 10.1039/F29767201525.
(30) Leung, S. C. E.; Wanninayake, D.; Chen, D.; Nguyen, N.-T.; Li, Q. Physicochemical properties and interactions of perfluoroalkyl substances (PFAS) - Challenges and opportunities in sensing and remediation. *Sci. Total Environ.* **2023**, *905*, 166764. DOI: 10.1016/j.scitotenv.2023.166764.
(31) Krafft, M. P.; Riess, J. G. Chemistry, Physical Chemistry, and Uses of Molecular Fluorocarbon−Hydrocarbon Diblocks, Triblocks, and Related Compounds—Unique "Apolar"

Components for Self-Assembled Colloid and Interface Engineering. *Chem. Rev.* **2009**, *109* (5), 1714-1792. DOI: 10.1021/cr800260k.
(32) Hasegawa, T. Physicochemical Nature of Perfluoroalkyl Compounds Induced by Fluorine. *The Chemical Record* **2017**, *17* (10), 903-917. DOI: 10.1002/tcr.201700018.
(33) Maibaum, L.; Dinner, A. R.; Chandler, D. Micelle Formation and the Hydrophobic Effect. *J. Phys. Chem. B* **2004**, *108* (21), 6778-6781. DOI: 10.1021/jp037487t.
(34) Nagarajan, R. Molecular Packing Parameter and Surfactant Self-Assembly: The Neglected Role of the Surfactant Tail. *Langmuir* **2002**, *18* (1), 31-38. DOI: 10.1021/la010831y.
(35) Tanford, C. *The hydrophobic effect: formation of micelles and biological membranes 2d ed*; J. Wiley., 1980.
(36) Sadtler, V. M.; Giulieri, F.; Krafft, M. P.; Riess, J. G. Micellization and Adsorption of Fluorinated Amphiphiles: Questioning the 1 CF2≈1.5 CH2 Rule. *Chem. Eur. J.* **1998**, *4* (10), 1952-1956. DOI: 10.1002/(SICI)1521-3765(19981002)4:10<1952::AID-CHEM1952>3.0.CO;2-V.
(37) Shinoda, K.; Hato, M.; Hayashi, T. Physicochemical properties of aqueous solutions of fluorinated surfactants. *J. Phys. Chem.* **1972**, *76* (6), 909-914. DOI: 10.1021/j100650a021.